

Network Behavioral-Feedback SIR Epidemic Model

Martina Alutto ^{a,c,*}, Leonardo Cianfanelli ^a, Giacomo Como ^{a,b}, Fabio Fagnani ^a

^a*Department of Mathematical Sciences “G.L. Lagrange,” Politecnico di Torino, 10129 Torino, Italy*

^b*Department of Automatic Control, Lund University, 22100 Lund, Sweden.*

^c*Institute of Electronics, Computer and Telecommunication Engineering, National Research Council of Italy, Politecnico di Torino, 10129 Torino, Italy*

Abstract

We propose a network behavioral-feedback Susceptible-Infected-Recovered (SIR) epidemic model in which the interaction matrix describing the infection rates across subpopulations depends in feedback on the current epidemic state. This model captures both heterogeneities in individuals’ mixing, contact frequency, aptitude to contract and spread the infection, and endogenous behavioral responses such as voluntary social distancing and the adoption of self-protective measures.

We study the stability of the equilibria and illustrate through several examples how the shape of the stability region depends on the structure of the interaction matrix, providing insights for the design of effective control strategies. We then analyze the transient behavior of the dynamics, showing that, for a special class of rank-1 interaction matrices, there always exists an aggregate infection curve that exhibits a unimodal behavior, expanding the results on the unimodality of infection curve known in the literature of epidemic models and paving the way for future control applications.

Key words: Network epidemics model, stability, behavioral-feedback

1 Introduction

Mathematical models play a central role in forecasting the spread of infectious diseases and guiding effective public health interventions. Among these, compartmental models are widely used for the analysis and control of epidemic outbreaks. One of the most studied compartmental models is the Susceptible-Infected-Recovered (SIR) epidemic model, see [Diekmann & Heesterbeek \(2000\)](#), [Hethcote \(2000\)](#), [Kermack & McKendrick \(1927\)](#), [McKendrick \(n.d.\)](#). In the SIR epidemic model the population is split into three compartments: *susceptible* agents who have not yet been infected, *infected* agents who carry the pathogen and can transmit the disease, and *recovered* agents, who have healed and gained immunity. The classical SIR model has served as

a foundation for many recent control strategies, including those developed during the COVID-19 pandemic, see, e.g., [Cianfanelli et al. \(2021\)](#), [Miclo et al. \(2022\)](#).

However, the classical SIR model relies on homogeneity assumptions regarding the pattern of contacts and the transmission rate that are often unrealistic. To address these limitations, network-based epidemic models have been proposed and analyzed in the last years as in [Paré et al. \(2020\)](#), [Pastor-Satorras et al. \(2015\)](#), [Zino & Cao \(2021\)](#). In these models, the nodes of the network represent different subpopulations of indistinguishable agents that may differ in several aspects, such as geographical area or age, e.g. in [Fall et al. \(2007\)](#), [Hethcote \(1978\)](#), [Mei et al. \(2017\)](#), [Nowzari et al. \(2016\)](#), [Ogura & Preciado \(2016\)](#). These subpopulations interact through a network, whose links represent the pattern of contacts. The *interaction matrix* A encodes the infection rate across the subpopulations, taking into account factors such as different susceptibility and infectivity levels of the subpopulations, and different interaction rates among them.

Most of the literature on networked epidemic models has focused on the Susceptible-Infected-Susceptible (SIS) epidemic model, where the agents do not acquire immunity after recovering from the disease. The seminal

* Corresponding author: Martina Alutto.

This work was partially supported by the Research Project PRIN 2022 “Extracting Essential Information and Dynamics from Complex Networks” (Grant Agreement number 2022MBC2EZ) funded by the Italian Ministry of University and Research.

Email addresses: martina.alutto@polito.it (Martina Alutto), leonardo.cianfanelli@polito.it (Leonardo Cianfanelli), giacomo.como@polito.it (Giacomo Como), fabio.fagnani@polito.it (Fabio Fagnani).

work by [Lajmanovich & Yorke \(1976\)](#) established a key bifurcation result: when the largest eigenvalue of A is below a threshold, the disease-free equilibrium is stable; otherwise, the system admits an endemic equilibrium. Many extensions of the network SIS model have been then studied, including models with higher-order interactions [Cisneros-Velarde & Bullo \(2021\)](#) and competing viruses [Anderson & Ye \(2023\)](#), [Liu et al. \(2019\)](#).

The *network SIR epidemic model* has been the subject of both numerical and theoretical studies, due to its relevance in capturing the spread of epidemics across subpopulations while accounting for recovery-induced immunity. On the numerical side, networked SIR models have been used to evaluate the effectiveness of targeted interventions, for instance to demonstrate that age-specific lockdown policies outperform uniform lockdown policies in reducing mortality and sustaining economic activity, even in simplified settings with two nodes only [Acemoglu et al. \(2021\)](#). From a theoretical perspective, several works have investigated the network SIR model [Alutto et al. \(2025\)](#), [Ellison \(2020\)](#), [Mei et al. \(2017\)](#). Of particular interest is the analysis when the interaction matrix is rank-1, which corresponds to assuming that the interaction rate between two subpopulations is proportional to the activity rate of the two subpopulations, without considering homophily [Alutto et al. \(2025\)](#), [Ellison \(2020\)](#), [Hethcote & Yorke \(2014\)](#). In particular, [Ellison \(2020\)](#) studied the case of symmetric rank-1 interaction matrix (corresponding to a uniform size, infectivity level, and susceptibility level of the subpopulations), providing, among other contributions, a characterization of the set of stable equilibria of the model that depends on the heterogeneity of the activity rates of the subpopulations. The analysis of the network SIR model has been largely enriched in [Alutto et al. \(2025\)](#), where the authors provided a rich set of theoretical results for the case of rank-1 asymmetric interaction matrix with n nodes. These results include the identification of n invariants of motion, conditions for the stability of the equilibria, a detailed analysis of transient dynamics at the single node level revealing the emergence of multimodal behaviors of the infection curves of single nodes, and the existence of a weighted aggregate infection curve that exhibits a unimodal behavior.

Besides the assumption of homogeneous population, another key limitation of the classical SIR model is the assumption of a constant transmission rate, which ignores the fact that typically the agents react to the spread of the epidemic and adapt their behavior accordingly [Crosby \(2003\)](#), [Lau et al. \(2005\)](#). An approach to overcome this limitation is to consider *behavioral-feedback epidemic models*, which incorporate the human endogenous behavior by letting the infection rate depend in feedback on the current epidemic state [Funk et al. \(2010\)](#), [Verelst et al. \(2016\)](#). The first feedback epidemic model was introduced in [Capasso & Serio \(1978\)](#), where the authors showed that, if the infection rate is a decreasing function of the fraction of infected agents,

the infection curve remains unimodal as in the classical SIR model. Subsequent studies demonstrated analytically that neglecting the human endogenous behavior may lead to mistakes in forecasting the trajectory of the epidemic, as the presence of feedback mechanisms can reduce the peak of the infection curve [Baker \(2020\)](#), [Franco \(2020\)](#), [Gao et al. \(2024\)](#). Some models extended the analysis by allowing the transmission rate to depend on both the fraction of susceptible and infected agents [Korobeinikov \(2006\)](#). In particular, [Alutto et al. \(2021\)](#) proved that the unimodality persists even when the infection rate depends jointly on the fraction of susceptible and infected agents, if the infection rate is non-decreasing in the fraction of susceptible agents.

An alternative approach to incorporate the human behavior is to introduce additional dynamic variables, e.g., to include strategic decision-making such as whether to vaccinate or adopt social distancing based on perceived risk and peer influence [Certório et al. \(2022\)](#), [Martins et al. \(2023\)](#), or to integrate opinion dynamics to model how the agents' beliefs about the epidemic influence adherence to protective measures [Paarporn et al. \(2017\)](#), [She et al. \(2022\)](#), [Xu & Ishii \(2024\)](#), [Xuan et al. \(2020\)](#), or to model how the infection rate depends on the perceived infection prevalence [Bizyaeva et al. \(2024\)](#), [Zhou et al. \(2020\)](#). The infection rate then depends on these additional variables, whose dynamics is coupled with the epidemic. However, these models are often too complicated to find analytical solutions to optimal control problems, and typically in the literature it is only characterized the stability of the equilibria and the asymptotic behavior of these models, e.g., to show emergence of oscillations that are not observed in standard epidemic models [Amaral et al. \(2021\)](#), [Frieswijk et al. \(2022\)](#), [Kabir & Tanimoto \(2020\)](#), [Paarporn & Eksin \(2023\)](#), [Ye et al. \(2021\)](#).

The analysis of SIR epidemic models that incorporate both network effects and behavioral adaptations remains limited and primarily empirical [Bisin & Moro \(2022\)](#), [Nemati Fard et al. \(2025\)](#), [Wang & Yao \(2025\)](#), with the exception of [Wang et al. \(2024\)](#), which introduces a variant of the network SIR model with a saturated incidence rate and a nonlinear recovery rate. The contribution of our paper is three-fold. First, we propose a network SIR model with behavioral-feedback mechanism (NBF-SIR model in short). In this model, the interaction matrix depends in feedback on the current epidemic state, capturing adaptive contact patterns and heterogeneous behavioral responses across subpopulations, such as voluntary social distancing, behavioral fatigue, or policy-driven restrictions. Second, we derive conditions for the stability of the equilibria, and explore how different functional forms of the interaction matrix influence the shape of the stability region. These findings underscore the importance of incorporating behavioral feedbacks in epidemic models and offer insights for the design of effective and targeted control strategies that aim to steer the system towards stable equilibria while minimizing the overall

fraction of agents that are infected throughout the outbreak. Third, for a special class of directed rank-1 interaction matrices, we establish the existence of a weighted aggregate infection curve that exhibits a unimodal behavior, generalizing the unimodality of the aggregate infection curve established in [Alutto et al. \(2025\)](#) for rank-1 network SIR model with constant interaction matrix. Since the unimodality of the infection curve is at the basis of the solution of several optimal control problems [Miclo et al. \(2022\)](#), this result paves the way for future control applications, which are left for future research.

The rest of the paper is organized as follows. In Section 2 we introduce the NBF-SIR model and provide some preliminary results. In Section 3 we study the stability of the equilibria and analyze the shape of the stability region for different interaction matrices. Section 4 focuses on the transient behavior of the dynamics proving that, for a special class of rank-1 interaction matrices, the dynamics exhibits a unimodal aggregate infection curve. Finally, Section 5 summarizes the work and discusses future research lines.

1.1 Notation

We briefly gather here some notational conventions adopted throughout the paper. We denote by \mathbb{R} and \mathbb{R}_+ the sets of real and nonnegative real numbers, respectively. The all-1 vector and the all-0 vector are denoted by $\mathbf{1}$ and $\mathbf{0}$, respectively, whose size may be deduced from the context. The spectrum of a matrix A is denoted $\sigma(A)$, and the transpose matrix is denoted A^T . For an irreducible matrix A in $\mathbb{R}_+^{n \times n}$, we let $\lambda_{max}(A)$ and $v_{max}(A)$ denote respectively the dominant eigenvalue of A and the corresponding left eigenvector normalized in such a way that $\mathbf{1}^T v_{max}(A) = 1$, which has positive entries and is unique due to the Perron-Frobenius theorem. For x in \mathbb{R}^n , we let $[x]$ denote the diagonal matrix whose diagonal coincides with x . Inequalities between two vectors x and y in \mathbb{R}^n are meant to hold true entry-wise, i.e., $x \leq y$ means that $x_i \leq y_i$ for every i , whereas $x < y$ means that $x_i < y_i$ for every i , and $x \lesssim y$ means that $x_i \leq y_i$ for every i and $x_j < y_j$ for some j . The same is meant to hold true for matrices in $\mathbb{R}^{n \times n}$. The real part of a complex number x is denoted by $\Re(x)$.

2 Model definition

In this section, we introduce the *network behavioral-feedback SIR epidemic model* (NBF-SIR), a generalization of the network SIR model [Alutto et al. \(2025\)](#), [Mei et al. \(2017\)](#) that incorporates an endogenous behavioral response to the epidemic. This model also extends the one presented in [Alutto et al. \(2021\)](#), where a scalar SIR model with endogenous behavioral response was examined, by incorporating a network structure.

We consider a system of $n \geq 1$ interacting subpopulations of indistinguishable agents. We let $x_i(t)$, $y_i(t)$, and $z_i(t)$ denote respectively the fraction of susceptible, infected, and recovered agents in each subpopulation $i = 1, \dots, n$ at time t , so that $x_i(t) + y_i(t) + z_i(t) = 1$

for every node i and time t . Due the normalization, we shall denote by (x, y) the state of the system and omit z without loss of generality. Every subpopulation is represented by a node of a network $\mathcal{G} = (\mathcal{V}, \mathcal{E}, A)$. The novelty of this model compared to [Alutto et al. \(2025\)](#) is that the *interaction matrix* $A : [0, 1]^{2n} \rightarrow \mathbb{R}_+^{n \times n}$ is a \mathcal{C}^1 function of the epidemic state (x, y) . The (i, j) -th entry of the interaction matrix $A_{ij}(x, y)$ accounts for the infection rate from subpopulation j to subpopulation i , which is modulated by the current epidemic state. This dependence allows to model several behavioral adaptations, e.g., a reduction of interactions with highly infected groups, thereby embedding a feedback mechanism between epidemic prevalence and social interaction patterns. Finally, $\gamma > 0$ models the recovery rate, which is assumed to be homogeneous across the network.

The NBF-SIR epidemic model with interaction matrix $A : [0, 1]^{2n} \rightarrow \mathbb{R}_+^{n \times n}$ and recovery rate $\gamma > 0$ is then the autonomous system of ordinary differential equations

$$\begin{cases} \dot{x}_i = -x_i \sum_j A_{ij}(x, y) y_j \\ \dot{y}_i = x_i \sum_j A_{ij}(x, y) y_j - \gamma y_i, \end{cases} \quad i = 1, \dots, n, \quad (1)$$

which, more compactly, reads

$$\dot{x} = -[x]A(x, y)y, \quad \dot{y} = [x]A(x, y)y - \gamma y. \quad (2)$$

Example 1 Consider the class of models with interaction matrix

$$A_{ij}(x, y) = g_i(x_i) f_j(y_j), \quad i, j = 1, \dots, n, \quad (3)$$

with $g_i, f_j : [0, 1] \rightarrow [0, \infty)$, for every $i, j = 1, \dots, n$. This model extends the network SIR model with asymmetric rank-1 interaction matrix considered in [Alutto et al. \(2025\)](#), by letting the interaction matrix A depend in feedback on the epidemic state. In this model, $g_i(x_i)$ accounts for the susceptibility level and activity rate of subpopulation i and $f_j(y_j)$ accounts for the infectivity level, activity rate and size of subpopulation j . This class of feedbacks is termed local to indicate that g_i depends only on the i -th component of x and f_j depends only on the j -th component of y . A special case of interaction matrix (3) is given by

$$A_{ij} = \frac{g_i(x_i)}{1 + \alpha y_j} \quad \forall i, j = 1, \dots, n, \quad (4)$$

where $g_i : [0, 1] \rightarrow [0, \infty)$ is an arbitrary non-decreasing function and $\alpha \geq 0$. This formulation models the idea that agents of subpopulation i tend to reduce their activity rate as the fraction of agents of subpopulation i that are currently infected or have been infected increases, because of an increased risk perception. On the other hand, the monotonicity with respect to y_j may capture how agents in other subpopulations tend to reduce the interactions

with agents of subpopulation j (or agents of subpopulation j tend to self-regulate their activity rate) as the fraction of infected agents in subpopulation j increases. This model generalizes previous scalar formulations provided in Baker (2020), Franco (2020) by incorporating a dependence on the fraction of susceptible agents and network effects.

The following result gathers some basic properties of the NBF-SIR epidemic model. To formalize the result properly, let

$$\mathcal{S} = \{(x, y) \in [0, 1]^{2n} : x + y \leq \mathbf{1}\}$$

denote the space of feasible states.

Proposition 2 Consider the NBF-SIR epidemic model (2) with \mathcal{C}^1 interaction matrix $A : [0, 1]^{2n} \rightarrow \mathbb{R}_+^{n \times n}$ and recovery rate $\gamma > 0$. Then:

- (i) for every initial condition $(x(0), y(0))$ in \mathcal{S} , there exists a unique solution $(x(t), y(t))$, which is \mathcal{C}^1 and belongs to \mathcal{S} for every t in \mathbb{R}_+ ;
- (ii) for every $i = 1, \dots, n$, $x_i(t)$ is non-increasing for $t \geq 0$, and $x_i(0) > 0$ if and only if $x_i(t) > 0$ for every $t \geq 0$;
- (iii) for every $i = 1, \dots, n$, if $y_i(0) > 0$, then $y_i(t) > 0$ for every $t > 0$;
- (iv) the set of equilibrium points in \mathcal{S} is

$$\mathcal{S}^* = \{(x^*, \mathbf{0}) : x^* \in [0, 1]^n\};$$

- (v) there exists x^* in \mathbb{R}_+^n such that $\mathbf{0} \leq x^* \leq x(0)$ and

$$\lim_{t \rightarrow +\infty} (x(t), y(t)) = (x^*, \mathbf{0}) \in \mathcal{S}^*. \quad (5)$$

PROOF. See Appendix A.

3 Stability of the equilibrium points

In this section, we analyze the stability properties of the NBF-SIR epidemic model (2). We first establish our main result, and then discuss its implications.

Theorem 3 Consider the NBF-SIR epidemic model (2) with \mathcal{C}^1 interaction matrix $A : [0, 1]^{2n} \rightarrow \mathbb{R}_+^{n \times n}$ and recovery rate $\gamma > 0$. Let $(x^*, \mathbf{0})$ in \mathcal{S}^* be an equilibrium point. Then:

- (i) if
$$\lambda_{\max}([x^*]A(x^*, \mathbf{0})) > \gamma, \quad (6)$$

then $(x^*, \mathbf{0})$ is unstable;

- (ii) if
$$\lambda_{\max}([x^*]A(x^*, \mathbf{0})) < \gamma, \quad (7)$$

then $(x^*, \mathbf{0})$ is stable.

PROOF. The Jacobian matrix of (2) evaluated in an equilibrium point $(x^*, \mathbf{0})$ in \mathcal{S}^* is

$$J(x^*, \mathbf{0}) = \begin{bmatrix} 0 & -[x^*]A(x^*, \mathbf{0}) \\ 0 & [x^*]A(x^*, \mathbf{0}) - \gamma \mathbf{I} \end{bmatrix}. \quad (8)$$

Hence, its spectrum is given by

$$\sigma(J(x^*, \mathbf{0})) = \sigma([x^*]A(x^*, \mathbf{0}) - \gamma \mathbf{I}) \cup \{0\}.$$

- (i) If Equation (6) holds true, then we have that

$$\max\{\Re(\lambda) : \lambda \in \sigma(J(x^*, \mathbf{0}))\} > 0.$$

Hence, by the linearization theorem, the equilibrium point $(x^*, \mathbf{0})$ is unstable.

- (ii) If Equation (7) holds true, then we have that

$$\max\{\Re(\lambda) : \lambda \in \sigma(J(x^*, \mathbf{0}))\} = 0.$$

In this case, the linearization theorem does not allow us to determine whether the equilibrium point is stable or unstable and we rely on the center manifold method (Guckenheimer & Holmes 1983, Section 3.2). For, observe that the center subspace for the equilibrium point $(x^*, \mathbf{0})$ is $\mathcal{V}_C = \{(x, \mathbf{0}) : x \in \mathbb{R}^n\}$. Since by Proposition 2(iv) the set of equilibrium points is given by $\mathcal{S}^* = \{(x, \mathbf{0}) : x \in [0, 1]^n\}$, we have that the center manifold coincides with \mathcal{S}^* itself. The reduced equation on this manifold is simply given by $\dot{x} = 0$, which implies that x^* is a stable equilibrium point for the reduced system. Therefore, stability of the equilibrium point $(x^*, \mathbf{0})$ for the NBF-SIR epidemic model (2) follows from the center-manifold theorem. ■

The next result provides sufficient conditions for the monotonicity of stability condition (7).

Proposition 4 Consider the NBF-SIR epidemic model (2) with \mathcal{C}^1 interaction matrix $A : [0, 1]^{2n} \rightarrow \mathbb{R}_+^{n \times n}$ and recovery rate $\gamma > 0$. If the following conditions hold:

$$A_{ij} + x_i \frac{\partial A_{ij}}{\partial x_i} \geq 0, \quad (9)$$

$$\frac{\partial A_{ij}}{\partial x_k} \geq 0 \quad (10)$$

for every i, j and k such that $k \neq i$, then the stability condition of the equilibrium $(x^*, \mathbf{0})$ given by (7) is monotone.

PROOF. From conditions (9)-(10), it follows that

$$\frac{\partial}{\partial x} [x]A(x, \mathbf{0}) \geq 0. \quad (11)$$

Therefore, for any x, z in $[0, 1]^n$ such that $x \leq z$, we get

$$[x]A(x, \mathbf{0}) \leq [z]A(z, \mathbf{0}). \quad (12)$$

Recalling a standard property of nonnegative square matrices, such that if $B \leq C$ entry-wise, then $\lambda_{\max}(B) \leq \lambda_{\max}(C)$ Meyer (2000), we obtain that

$$\lambda_{\max}([x]A(x, \mathbf{0})) \leq \lambda_{\max}([z]A(z, \mathbf{0})). \quad (13)$$

This implies that if the equilibrium $(z, \mathbf{0})$ is stable, then every equilibrium of the form $(x, \mathbf{0})$ with $x \leq z$ is also stable. ■

We now define the *stability region* \mathcal{S}^{**} of the NBF-SIR model (2) by

$$\mathcal{S}^{**} = \{(x, \mathbf{0}) \in \mathcal{S}^* : (7)\},$$

coinciding with the set of stable equilibrium points as per Theorem 3. Under the assumption that the subpopulations have equal size (the definition can be adapted if the subpopulations have different size), the set

$$\mathcal{X} = \operatorname{argmax}_{\substack{x \in [0,1]^n \\ (x,y) \in \overline{\mathcal{S}^{**}}}} \frac{1}{n} \sum_{j=1}^n x_j$$

identifies the points inside the closure of the stability region that maximize the fraction of susceptible agents. Note that \mathcal{X} belongs to the boundary of \mathcal{S}^{**} by construction. Identifying the stability region and the set \mathcal{X} is crucial to design effective control strategies. Indeed, in optimal control problems with infinite time horizons, the cost of control policies that do not steer the system towards stable equilibria diverges in time [Cianfanelli et al. \(2021\)](#). Hence, a sustainable control policy should drive the system toward a stable equilibrium with as large as possible fraction of susceptible agents, that is, in the stability region and as close as possible \mathcal{X} , to minimize the overall spread of the infection while ensuring long-term stability. The set \mathcal{X} was first informally introduced in [Ellison \(2020\)](#) to discuss the effects of heterogeneity when a planner aims to design a control that drives the system toward stable equilibria that maximize the fraction of susceptible agents in the network SIR model with no feedback and with rank-1 symmetric interaction matrices. The next examples illustrate the stability regions of several NBF-SIR models.

Example 5 Consider the NBF-SIR model (2) with $n = 2$ nodes, no feedback, interaction matrix

$$A = \begin{bmatrix} a & b \\ c & d \end{bmatrix}. \quad (14)$$

and recovery rate $\gamma = 1$. The stability region is determined by $\lambda_{\max}([x]A(x, 0))$, which reads

$$\frac{ax_1 + dx_2}{2} + \sqrt{\left(\frac{ax_1 + dx_2}{2}\right)^2 - \Delta x_1 x_2},$$

where $\Delta = ad - bc$ is the determinant of the interaction matrix. When A is rank-1, i.e., when $\Delta = 0$, the stability region \mathcal{S}^{**} is the intersection between $[0, 1]^2$ and a half plane. An example is shown in Figure 1(a) with

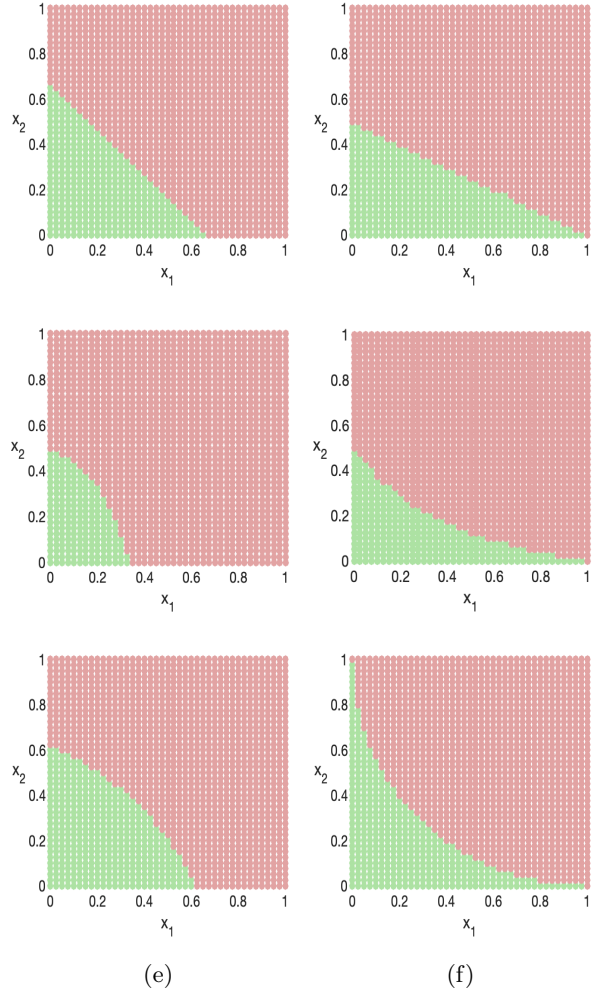


Fig. 1. Stability region of two nodes NBF-SIR epidemic models with different interaction matrices.

$A = 1.5\mathbf{1}\mathbf{1}^T$. This special case corresponds to an arbitrary partition of a homogeneous population into two subpopulations. In this case, every point on the boundary of \mathcal{S}^{**} belongs to \mathcal{X} , meaning that the planner should drive the system as close as possible to the boundary of \mathcal{S}^{**} and all such points are equivalent, which is not surprising, since the model is essentially equivalent to a scalar SIR model. In contrast, Figure 1(b) illustrates the stability region with interaction matrix (14) and $a = c = 1$, $b = d = 2$, which models two subpopulations with different infectivity levels. Due to this heterogeneity, \mathcal{X} is the singleton that contains the maximally asymmetric equilibrium on the boundary of \mathcal{S}^{**} where all agents that have been infected and are now recovered belong to the most infective subpopulation. When A is not rank-1, the geometry of \mathcal{S}^{**} depends on the sign of Δ . If $\Delta > 0$, which is typically associated with homophily (i.e., agents tend to interact more within their own group), explicit computation shows that \mathcal{S}^{**} is a convex region. Conversely, if $\Delta < 0$, indicating predominant inter-groups interactions, then $[0, 1]^2 \setminus \mathcal{S}^{**}$ is convex. These scenarios are

illustrated in Figure 1(c) for the rank-2 matrix (14) with $a = 3, b = 2, c = 1, d = 2$ and in Figure 1(d) for the rank-2 matrix (14) with $a = 1, b = 2, c = 3, d = 2$, respectively. The shape of \mathcal{S}^{**} in turn determines the structure of \mathcal{X} and the equilibria that the planner should target.

Example 6 Consider the NFB-SIR model (2) with

$$A_{ij}(x, y) = \frac{1 + x_i}{1 + \alpha y_j}, \quad \alpha \geq 0, i, j = 1, \dots, n.$$

This model fits with (4), as $A(x, y)$ is rank-1 matrix with local feedback. In this model, the agents increase their activity rate in response to a higher fraction of susceptible agents in their subpopulation. Using the fact that A is rank-1, we get that

$$\lambda_{\max}([x]A(x, \mathbf{0})) = \sum_{i=1}^n x_i(1 + x_i),$$

hence the stability region \mathcal{S}^{**} is convex. Figure 1(e) illustrates the stability region with $n = 2, \alpha = 1.5$ and $\gamma = 1$. The convexity of the stability region and the symmetry of A imply that \mathcal{X} is the singleton that contains the maximally symmetric equilibrium on the boundary of the stability region, therefore the planner should drive the system in the stability region and as close as possible to such equilibrium.

Example 7 Consider the NFB-SIR model (2) with

$$A_{ij}(x, y) = \frac{2 - x_i}{1 + y_1 + y_2}, \quad i, j = 1, \dots, n.$$

In this case, $A_{ij}(x, y)$ decreases as the fraction of susceptible agents x_i increases, aligning with the progression of the fraction of agents of the same population that have been infected. This behavior may represent the effect of increasing pandemic fatigue, where agents progressively reduce their adherence to restrictive measures as the epidemic evolves and x_i decreases. Moreover, the feedback is non-local, since all entries of the interaction matrix depend on the entire vector y , which models situations where the agents are not aware of the subpopulation that other agents belong to. In this case,

$$\lambda_{\max}([x]A(x, \mathbf{0})) = \sum_{i=1}^n x_i(2 - x_i).$$

Figure 1(f) illustrates the stability region when $n = 2$ and $\gamma = 1$. The convexity of $[0, 1]^2 \setminus \mathcal{S}^{**}$ and the symmetry of A imply that \mathcal{X} contains the two maximally asymmetric equilibrium points on the boundary of the stability region. Hence, the planner should promote lockdown in a single population to drive the system as close as possible to these asymmetric equilibria where all agents that have been infected belong to the same population.

Remark 8 Note that, since all equilibria are disease-free and the stability of an equilibrium does not depend on the derivatives of the interaction matrix, the stability of an equilibrium $(x, \mathbf{0})$ depends only on $A(x, \mathbf{0})$. Therefore, the stability regions illustrated in Figure 1(e)-(f) apply to every interaction matrix such that $A_{ij}(x, \mathbf{0}) = 1 + x_i$ and $A_{ij}(x, \mathbf{0}) = 2 - x_i$, respectively.

Examples 5-7 show that, depending on the structure of the interaction matrix, the planner should drive the system towards different equilibria and design different control strategies accordingly. The analysis applies both to local and non-local feedback mechanisms, to full-rank matrices, and even to asymmetric feedback mechanisms considered in the literature, e.g., a subpopulation (*risk-aversers*) reducing their interactions as the infection spreads, similar to those who adhered to strict social distancing measures during the COVID-19 pandemic, and a second subpopulation (*risk-tolerators*) with negative feedback relative to the total fraction of susceptible agents [Bizyaeva et al. \(2024\)](#), [Zhou et al. \(2020\)](#).

4 Transient behavior of the NBF-SIR model

In the previous section we have discussed the stability properties of the NBF-SIR model and the implications of network effects and behavioral feedbacks for the design of control strategies. This section focuses on the transient behavior of the dynamics. The main result of the section is that, under some assumptions on the feedback mechanism, the NBF-SIR model with rank-1 interaction matrix considered in Example 1 admits an aggregate infection curve that exhibits a unimodal behavior. Note that the class of NBF-SIR models considered in Example 1 can be rewritten as

$$\begin{cases} \dot{x}_i = -x_i g_i(x_i) \sum_{j=1}^n f_j(y_j) y_j \\ \dot{y}_i = x_i g_i(x_i) \sum_{j=1}^n f_j(y_j) y_j - \gamma y_i \end{cases} \quad \forall i = 1, \dots, n. \quad (15)$$

For this model, the dominant eigenvalue of $A(x, y)$ is $g(x)^T f(y)$, corresponding to the trace of $A(x, y)$, with unique left dominant eigenvector $v_{\max}(A(x, y)) = f(y)$. Now, let

$$\bar{y}(t) = \sum_{j=1}^n f_j(y_j(t)) y_j(t). \quad (16)$$

The next result states that, under reasonable assumptions, $t \mapsto \bar{y}(t)$ is unimodal, namely, it exhibits a single peak.

Theorem 9 Consider model (15) with initial condition $(x(0), y(0))$ in \mathcal{S} such that

$$\mathbf{0} \preceq x(0) \leq \mathbf{1} - y(0) \preceq \mathbf{1}. \quad (17)$$

Assume that $g(x), f(y) > \mathbf{0}$, that $x_i g_i(x_i)$ is increasing and $f_j(y_j) y_j$ is increasing and concave for every $i, j = 1, \dots, n$ and (x, y) in \mathcal{S} . Then:

- (i) if $\dot{\bar{y}}(0) \leq 0$, then $\bar{y}(t)$ is strictly decreasing for $t \geq 0$;
- (ii) if $\dot{\bar{y}}(0) > 0$, then there exists $\hat{t} > 0$ such that $\bar{y}(t)$ is strictly increasing on $[0, \hat{t}]$ and strictly decreasing on $[\hat{t}, +\infty)$.

PROOF. (i) We prove the result by contradiction. If (i) does not hold true, there must exist $\tau \geq 0$ such that $\dot{\bar{y}}(\tau) = 0$ and $\ddot{\bar{y}}(\tau) \geq 0$. Direct computation yields

$$\begin{aligned}\dot{\bar{y}} &= \sum_{j=1}^n \dot{y}_j [f'_j y_j + f_j], \\ \ddot{\bar{y}} &= \sum_{j=1}^n [f''_j y_j + 2f'_j] \dot{y}_j^2 + \sum_{j=1}^n [f'_j y_j + f_j] \ddot{y}_j\end{aligned}\quad (18)$$

where, from (15),

$$\ddot{y}_j = \dot{x}_j g_j \bar{y} + x_j g'_j \dot{x}_j \bar{y} + x_j g_j \ddot{y} - \gamma \dot{y}_j \quad (19)$$

for every $j = 1, \dots, n$. For simplicity of notation, we omit the dependence on τ on the right-hand side of the following equation. Note that

$$\begin{aligned}\ddot{\bar{y}}(\tau) &\leq \sum_{j=1}^n (f'_j y_j + f_j) \ddot{y}_j \\ &\leq \bar{y} \sum_{j=1}^n (f'_j y_j + f_j) (g'_j x_j + g_j) \dot{x}_j - \gamma \dot{\bar{y}} \\ &= \bar{y} \sum_{j=1}^n (f'_j y_j + f_j) (g'_j x_j + g_j) \dot{x}_j,\end{aligned}\quad (20)$$

where the first inequality follows from the second equation of (18) and from concavity of $f_j(y_j)y_j$, while the second one follows from (19), from the first equation of (18) and from $\dot{\bar{y}}(\tau) = 0$. Now, note that $x_j g_j(x_j)$ and $f_j(y_j)y_j$ are both increasing for every $j = 1, \dots, n$, hence

$$\begin{aligned}f'_j(y_j(\tau))y_j(\tau) + f_j(y_j(\tau)) &> 0, \\ g'_j(x_j(\tau))x_j(\tau) + g_j(x_j(\tau)) &> 0.\end{aligned}\quad (21)$$

Moreover, since $y(0) \succeq \mathbf{0}$ and $f(y) > \mathbf{0}$, Proposition 2(iii) implies that

$$\bar{y}(\tau) > 0. \quad (22)$$

Furthermore,

$$\dot{x}_j(\tau) < 0 \text{ for } a \text{ } j \in \{1, \dots, n\}. \quad (23)$$

This follows from $x(0) \succeq \mathbf{0}$ and from Proposition 2(ii), which implies that $x_j(\tau) > 0$ for at least a $j = 1, \dots, n$. Hence, $\dot{x}_j(\tau) < 0$ is implied by $\bar{y}(\tau) > 0$, $g(x) > \mathbf{0}$ and (15). Plugging (21)-(23) into (20) we get a contradiction and prove the statement.

(ii) Assume by contradiction that $\dot{\bar{y}}(t) > 0$ for every $t \geq 0$. This would imply the existence of a node j such that

$\dot{y}_j(t) > 0$ for all $t \geq 0$, contradicting Proposition 2(v). Hence, $\hat{t} = \min\{t \geq 0 : \dot{\bar{y}}(t) = 0\}$ is well defined and $\bar{y}(t)$ is increasing in $[0, \hat{t}]$. The fact that \bar{y} is decreasing for $t > \hat{t}$ follows from point (i). ■

Remark 10 Let $h_{ij}(x_i, y_j) = x_i g_i(x_i) f_j(y_j) y_j$ denote the force of infection from node j to node i , which represents the rate of new infections in subpopulation i due to interactions with infected agents of subpopulation j . The assumptions of Theorem 9 have a clear epidemiological motivation as they can be equivalently expressed in terms of $h_{ij}(x_i, y_j)$ by saying that $h_{ij}(x_i, y_j)$ is increasing in x_i and y_j and concave in y_j . The monotonicity of $h_{ij}(x_i, y_j)$ with respect to y_j reflects the idea that more infected agents lead to a higher transmission rate, even though the per capita interactions of single infected agents may decrease due to behavioral adaptations. The concavity captures saturation effects, namely, when more agents are already infected, the impact of an additional one on the rate of new infections decreases. The monotonicity with respect to x_i reflects the idea that a larger susceptible population increases the potential for new infections. Note that interaction matrix (4) satisfies all assumptions of Theorem 9.

Remark 11 The unimodality of $\bar{y} = \sum b_j y_j$ was established in (Alutto et al. 2025, Theorem 1) for the network SIR model with constant rank-1 interaction matrix

$$A = ab^T$$

with vectors $a, b > \mathbf{0}$. Since for this constant interaction matrix the force of infection $h_{ij}(x_i, y_j) = a_i x_i b_j y_j$ is increasing in x_i and y_j and concave in y_j , and since in this case $f(y) = b$, Theorem 9 generalizes such a result.

Remark 12 The aggregate variable $\bar{y} = \sum_j f_j(y_j)y_j$ is increasing in every component y_j and may be interpreted as an indicator of the overall infection level in the network. In some special cases, e.g., with interaction matrix (4) with $\alpha = 0$ and when the subpopulations have equal size, $\bar{y} = \sum y_j$ is proportional to the fraction of infected agents in the entire population.

Example 13 Figure 2 illustrates a numerical simulation of the NBF-SIR epidemic model (15) with $n = 5$ subpopulations, interaction matrix $A(x, y) = 0.8(\mathbf{1} - x)y^T$ and $\gamma = 1$. This interaction matrix is rank-1, but $x_i g_i(x_i) = 0.8x_i(1 - x_i)$ is not increasing in x_i for every x_i in $[0, 1]$. As a result, the sufficient conditions established in Theorem 9 for the unimodality of the aggregate infection curve are not met. In fact, as illustrated in the figure, the aggregate infection curve exhibits a multimodal behavior. This example highlights that even in the presence of a rank-1 interaction matrix, the aggregate infection curve may in general exhibit multimodal behaviors.

5 Conclusion

In this work, we introduced the network behavioral-feedback SIR epidemic model (NBF-SIR), a networked

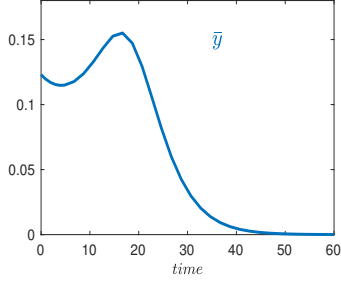


Fig. 2. Numerical simulation of the NBF-SIR model of Example 13.

SIR model where the interaction matrix depends in feedback on the epidemic state, to incorporate behavioral adaptations such as voluntary social distancing. We characterized the stability of the equilibria, and analyze how the structure of the interaction matrix affects the stability region. We then considered the transient of dynamics for rank-1 interaction matrices, showing that, under certain assumptions on the feedback mechanism, the dynamics admits a unimodal aggregate infection curve.

Future research directions include the analysis of the transient dynamics for matrices with higher rank, e.g., to include homophily and heterogeneous interactions, and the design of optimal control strategies for the NBF-SIR model that exploit the properties of the model that have been established in this paper.

A Proof of Proposition 2

(i) Since A is \mathcal{C}^1 , the vector field of (2) is \mathcal{C}^1 with respect to (x, y) . Hence, existence and uniqueness of the solution is a standard result (Hale 1980, Chapter I.3). To prove that \mathcal{S} is positively invariant, note that for every point belonging to the boundary of \mathcal{S} , the vector field is either tangent, or points inside the set \mathcal{S} . Therefore for $(x(0), y(0))$ in \mathcal{S} , it follows from Nagumo's Theorem Blanchini & Miani (2007) that $(x(t), y(t))$ belongs to \mathcal{S} for all $t > 0$, which means that \mathcal{S} is a positively invariant set.

(ii) Since \mathcal{S} is positively invariant, $x(t)$, $y(t)$ and $A(x(t), y(t))$ have non-negative entries for every time t . Therefore,

$$\dot{x}_i(t) = -x_i(t) \sum_{j=1}^n A_{ij}(x, y) y_j(t) \leq 0$$

for all $i = 1, \dots, n$ and $t \geq 0$. By integrating the first equation of (1), for each node i we get

$$x_i(t) = x_i(0) \exp\left(-\int_0^t \sum_{j=1}^n A_{ij}(x(\tau), y(\tau)) y_j(\tau) d\tau\right),$$

hence $x_i(t) > 0$ for every $t \geq 0$ if and only if $x_i(0) > 0$.

(iii) Since $\dot{y}_i(t) \geq -\gamma y_i(t)$, Gronwall's inequality implies $y_i(t) \geq y_i(0)e^{-\gamma t} > 0$.

(iv) A point $(x^*, y^*) \in \mathcal{S}$ is an equilibrium if and only if

$$\mathbf{0} = -[x^*]A(x^*, y^*)y^*, \quad \mathbf{0} = [x^*]A(x^*, y^*)y^* - \gamma y^*.$$

This implies that the points of the form $(x^*, \mathbf{0})$, are all equilibria, referred to as a *disease-free equilibria*. Moreover, these are the only equilibria, since every point with $y^* \neq \mathbf{0}$ would not satisfy the equilibrium conditions given above.

(v) Observe that the sum of the first two equations of (1) is $\dot{x}_i(t) + \dot{y}_i(t) = -\gamma y_i(t) \leq 0$ for every i , hence $x_i(t) + y_i(t)$ is a non-increasing function. Since $x_i(t)$ and $x_i(t) + y_i(t)$ are both non-increasing functions, they both admit a limit

$$x_i^* := \lim_{t \rightarrow +\infty} x_i(t), \quad \xi_i^* := \lim_{t \rightarrow +\infty} [x_i(t) + y_i(t)].$$

As a consequence, the following limit

$$y_i^* = \lim_{t \rightarrow +\infty} y_i(t) = \xi_i^* - x_i^* \geq 0$$

exists. Suppose now by contradiction that $y_i^* > 0$. This means that there exist $T, \epsilon > 0$ such that $y_i(t) > \epsilon$, for all $t \geq T$. Then, we get

$$\begin{aligned} \xi_i^* &= \lim_{t \rightarrow +\infty} [x_i(t) + y_i(t)] \\ &= x_i(0) + y_i(0) - \gamma \lim_{t \rightarrow +\infty} \int_0^t y_i(\tau) d\tau \\ &< x_i(0) + y_i(0) - \gamma \lim_{t \rightarrow +\infty} \int_T^t y_i(\tau) d\tau \\ &< x_i(0) + y_i(0) - \gamma \epsilon \lim_{t \rightarrow +\infty} (t - T) = -\infty \end{aligned}$$

As this is a contradiction, it must be $y_i^* = 0$ and this is valid for every $i = 1, \dots, n$. Therefore, for every $(x(0), y(0))$ in \mathcal{S} , the trajectory $(x(t), y(t))$ converges to an equilibrium of the form $(x^*, \mathbf{0})$. Moreover, from point (ii), it holds true $\mathbf{0} \leq x^* \leq x(0)$. ■

References

- Acemoglu, D., Chernozhukov, V., Werning, I. & Whinston, M. D. (2021), 'Optimal targeted lockdowns in a multigroup SIR model', *American Economic Review: Insights* **3**(4), 487–502.
- Alutto, M., Cianfanelli, L., Como, G. & Fagnani, F. (2025), 'On the dynamic behavior of the network SIR epidemic model', *IEEE Transactions on Control of Network Systems* **12** pp.(1), 177–189.
- Alutto, M., Como, G. & Fagnani, F. (2021), 'On SIR epidemic models with feedback-controlled interactions and network effects', *2021 60th IEEE Conference on Decision and Control (CDC 2021)* pp. 5562–5567.

- Amaral, M. A., Oliveira, M. M. & Javarone, M. A. (2021), ‘An epidemiological model with voluntary quarantine strategies governed by evolutionary game dynamics’, *Chaos, Solitons & Fractals* **143**, 110616.
- Anderson, B. D. O. & Ye, M. (2023), ‘Equilibria analysis of a networked bivirus epidemic model using Poincaré–Hopf and manifold theory’, *SIAM Journal on Applied Dynamical Systems* **22**(4), 2856–2889.
- Baker, R. (2020), ‘Reactive social distancing in a SIR model of epidemics such as COVID-19’, *arXiv preprint arXiv:2003.08285*.
- Bisin, A. & Moro, A. (2022), ‘Spatial-SIR with network structure and behavior: Lockdown rules and the lucas critique’, *Journal of Economic Behavior & Organization* **198**, 370–388.
- Bizyaeva, A., Arango, M. O., Zhou, Y., Levin, S. & Leonard, N. E. (2024), Active risk aversion in SIS epidemics on networks, in ‘2024 American Control Conference (ACC)’, IEEE, pp. 4428–4433.
- Blanchini, F. & Miani, S. (2007), *Set-Theoretic Methods in Control*.
- Capasso, V. & Serio, G. (1978), ‘A generalization of the Kermack–McKendrick deterministic epidemic model’, *Mathematical Biosciences* **42**(1), 43–61.
- Certório, J., Martins, N. C. & La, R. J. (2022), ‘Epidemic population games with nonnegligible disease death rate’, *IEEE Control Systems Letters* **6**, 3229–3234.
- Cianfanelli, L., Parise, F., Acemoglu, D., Como, G. & Ozdaglar, A. (2021), Lockdown interventions in the SIR model: Is the reproduction number the right control variable?, in ‘Proceedings of the 60th IEEE Conference on Decision and Control (CDC 2021)’, IEEE, pp. 4254–4259.
- Cisneros-Velarde, P. & Bullo, F. (2021), ‘Multigroup SIS epidemics with simplicial and higher order interactions’, *IEEE Transactions on Control of Network Systems* **9**(2), 695–705.
- Crosby, A. W. (2003), *America’s Forgotten Pandemic: The Influenza of 1918*, Cambridge University Press.
- Diekmann, O. & Heesterbeek, J. A. P. (2000), Mathematical epidemiology of infectious diseases: Model building, analysis and interpretation.
- Ellison, G. (2020), Implications of heterogeneous SIR models for analyses of covid-19, Working Paper 27373, National Bureau of Economic Research.
- Fall, A., Iggidr, A., Sallet, G. & Tewa, J. J. (2007), ‘Epidemiological models and Lyapunov functions’, *Math. Model. Nat. Phenom.* **2**(1), 62–83.
URL: <https://doi.org/10.1051/mmnp:2008011>
- Franco, E. (2020), ‘A feedback SIR (fSIR) model highlights advantages and limitations of infection-dependent mitigation strategies’, *arXiv preprint arXiv:2004.13216*.
- Frieswijk, K., Zino, L., Ye, M., Cao, M. & Rizzo, A. (2022), ‘A mean-field analysis of a network behavioural-epidemic model’, *IEEE Control Systems Letters* **6**, 2533–2538.
- Funk, S., Salathé, M. & Jansen, V. A. (2010), ‘Modelling the influence of human behaviour on the spread of infectious diseases: a review’, *Journal of the Royal Society Interface* **7**(50), 1247–1256.
- Gao, W., Wang, Y., Cao, J. & Liu, Y. (2024), ‘Final epidemic size and critical times for susceptible-infectious-recovered models with a generalized contact rate’, *Chaos* **34**(1), 013152.
- Guckenheimer, J. & Holmes, P. (1983), *Nonlinear Oscillations, Dynamical Systems, and Bifurcations of Vector Fields*, Vol. 42 of *Applied Mathematical Sciences*, Springer, New York, NY.
- Hale, J. K. (1980), *Ordinary Differential Equations*, 2nd edn, Robert E. Krieger Publishing Co., Inc., Huntington, N.Y.
- Hethcote, H. W. (1978), ‘An immunization model for a heterogeneous population’, *Theoretical population biology* **14**(3), 338–349.
- Hethcote, H. W. (2000), ‘The mathematics of infectious diseases’, *SIAM Rev.* **42**, 599–653.
- Hethcote, H. W. & Yorke, J. A. (2014), *Gonorrhoea transmission dynamics and control*, Vol. 56, Springer.
- Kabir, K. A. & Tanimoto, J. (2020), ‘Evolutionary game theory modeling to represent the behavioural dynamics of economic shutdowns and shield immunity in the COVID-19 pandemic’, *Royal Society Open Science* **7**(9), 201095.
- Kermack, W. O. & McKendrick, A. G. (1927), ‘A contribution to the mathematical theory of epidemics’, *Proceedings of the Royal Society of London. Series A* **115**(772), 700–721.
- Korobeinikov, A. (2006), ‘Lyapunov functions and global stability for SIR and SIRS epidemiological models with non-linear transmission’, *Bulletin of Mathematical biology* **68**, 615–626.
- Lajmanovich, A. & Yorke, J. A. (1976), ‘A deterministic model for gonorrhoea in a nonhomogeneous population’, *Mathematical Biosciences* **28**(3-4), 221–236.
- Lau, J. T., Yang, X., Pang, E., Tsui, H., Wong, E. & Wing, Y. K. (2005), ‘SARS-related perceptions in Hong Kong’, *Emerging infectious diseases* **11**(3), 417.
- Liu, J., Paré, P. E., Nedić, A., Tang, C., Beck, C. L. & Basar, T. (2019), ‘Analysis and control of a continuous-time bi-virus model’, *IEEE Transactions on Automatic Control* **64**(12), 4891–4906.
- Martins, N. C., Certório, J. & La, R. J. (2023), ‘Epidemic population games and evolutionary dynamics’, *Automatica* **153**, 111016.
- McKendrick, A. G. (n.d.), ‘Applications of mathematics to medical problems’, *Proceedings of the Edinburgh Mathematical Society* **44**, 98 – 130.
- Mei, W., Mohagheghi, S., Zampieri, S. & Bullo, F. (2017), ‘On the dynamics of deterministic epidemic propagation over networks’, *Annual Reviews in Control* **44**, 116–128.
- Meyer, C. D. (2000), *Matrix Analysis and Applied Linear Algebra*, SIAM, Philadelphia, PA.
- Miclo, L., Spiro, D. & Weibull, J. (2022), ‘Optimal epidemic suppression under an ICU constraint’, *Journal of Mathematical Economics* **101**, 102669.

- Nemati Fard, L. A., Bisin, A., Starnini, M., Tizzoni, M. et al. (2025), ‘Modeling adaptive forward-looking behavior in epidemics on networks’, *Journal of Economic Behavior & Organization* **232**, 106914.
- Nowzari, C., Preciado, V. M. & Pappas, G. J. (2016), ‘Analysis and control of epidemics: A survey of spreading processes on complex networks’, *IEEE Control Systems Magazine* **36**(1), 26–46.
- Ogura, M. & Preciado, V. M. (2016), ‘Stability of spreading processes over time-varying large-scale networks’, *IEEE Transactions on Network Science and Engineering* **3**, 44–57.
- Paarporn, K. & Eksin, C. (2023), SIS epidemics coupled with evolutionary social distancing dynamics, in ‘2023 American Control Conference (ACC)’, IEEE, pp. 2023–2028.
- Paarporn, K., Eksin, C., Weitz, J. S. & Shamma, J. S. (2017), ‘Networked SIS epidemics with awareness’, *IEEE Transactions on Computational Social Systems* **4**(3), 93–103.
- Paré, P. E., Beck, C. L. & Basar, T. (2020), ‘Modeling, estimation, and analysis of epidemics over networks: An overview’, *Annual Reviews in Control* **50**, 345–360.
- Pastor-Satorras, R., Castellano, C., Van Mieghem, P. & Vespignani, A. (2015), ‘Epidemic processes in complex networks’, *Reviews of Modern Physics* **87**, 925–979.
- She, B., Liu, J., Sundaram, S. & Paré, P. E. (2022), ‘On a networked SIS epidemic model with cooperative and antagonistic opinion dynamics’, *IEEE Transactions on Control of Network Systems* **9**(3), 1154–1165.
- Verelst, F., Willem, L. & Beutels, P. (2016), ‘Behavioural change models for infectious disease transmission: A systematic review (2010-2015)’, *Journal of The Royal Society Interface* **13**.
- Wang, F., Zhang, J. & Liu, M. (2024), ‘Dynamical analysis of a network-based SIR model with saturated incidence rate and nonlinear recovery rate: an edge-compartmental approach’, *Mathematical Biosciences and Engineering* **21**(4), 5430–5445.
- Wang, G. & Yao, W. (2025), ‘An application of complex networks on predicting the behavior of infectious disease on campus’, *Mathematical Methods in the Applied Sciences* **48**, 189–206.
- Xu, Q. & Ishii, H. (2024), ‘On a discrete-time networked SIV epidemic model with polar opinion dynamics’, *IEEE Transactions on Network Science and Engineering* **PP**, 1–16.
- Xuan, W., Ren, R., Paré, P. E., Ye, M., Ruf, S. F. & Liu, J. (2020), ‘On a network SIS model with opinion dynamics’, *IFAC-PapersOnLine* **53**, 2582–2587.
- Ye, M., Zino, L., Rizzo, A. & Cao, M. (2021), ‘Game-theoretic modeling of collective decision making during epidemics’, *Physical Review E* **104**(2), 024314.
- Zhou, Y., Levin, S. & Leonard, N. (2020), ‘Active control and sustained oscillations in actSIS epidemic dynamics’, *IFAC-PapersOnLine* **53**, 807–812.
- Zino, L. & Cao, M. (2021), ‘Analysis, prediction, and control of epidemics: A survey from scalar to dynamic network models’, *IEEE Circuits and Systems Maga-*